Volume 4
Number 3
7 February 2023
Pages 717–978

Materials Advances

rsc.li/materials-advances

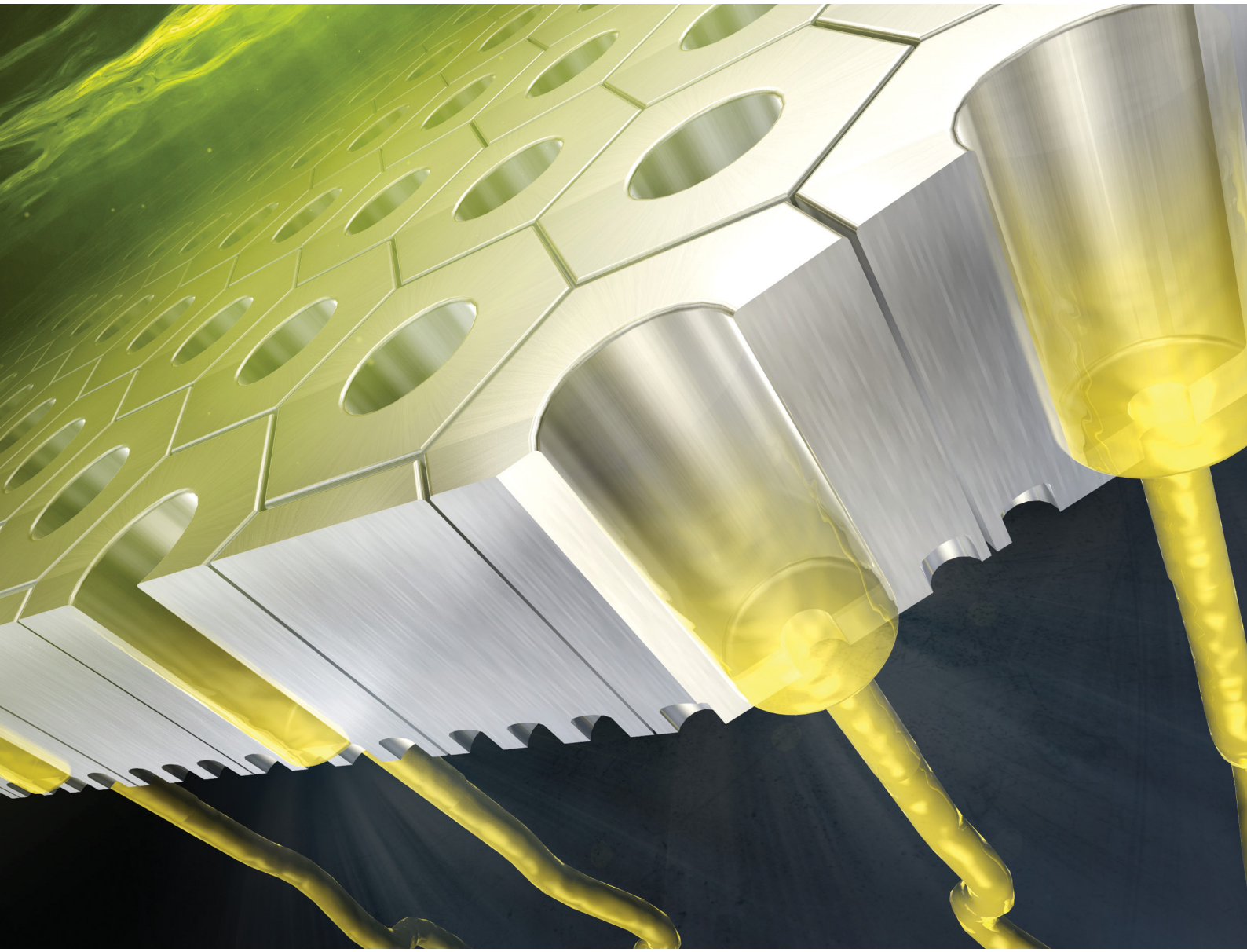

ISSN 2633-5409

ROYAL SOCIETY OF CHEMISTRY

PAPER

Takashi Yanagishita *et al.*

Continuous spinning of polymer nanofibers with uniform diameters using an anodic porous alumina spinneret with holes of different diameters

Materials Advances

ROYAL SOCIETY OF CHEMISTRY

PAPER

View Article Online
View Journal | View Issue

Cite this: *Mater. Adv.*, 2023, 4, 890

Continuous spinning of polymer nanofibers with uniform diameters using an anodic porous alumina spinneret with holes of different diameters

Takashi Yanagishita, * Akane Koga and Hideki Masuda

Monodisperse polymer nanofibers smaller than 50 nm were prepared *via* continuous spinning using anodic porous alumina as a spinneret. In the nanofiber spinning method using a spinneret, the diameter of the resulting nanofibers depends on the diameter of the spinneret aperture. Therefore, in order to spin fine nanofibers, it is necessary to use a spinneret with a fine aperture. However, as the aperture size decreases, the pressure loss in the direction of depth in the spinneret increases, making it difficult to extrude highly viscous polymer solutions. To overcome this problem, we have developed new types of anodic porous alumina spinnerets with holes of different diameters in the direction of its thickness. In the spinneret with holes of different diameters, the layer with fine holes acts as an aperture layer for extrusion of the polymer solution, and the layer with larger holes acts as a support layer. By adopting the spinneret with two-layered hole array structures, we can realize extrusion with low-pressure loss and a reduced hole diameter. Using this new type of spinneret, we can achieve the formation of extremely fine nanofibers of ~12 nm diameter. We also prepared fine carbon nanofibers through carbonization of the obtained nanofibers as a precursor. The obtained nanofibers are expected to be used in various applications.

Received 4th November 2022,
Accepted 31st December 2022

DOI: 10.1039/d2ma01017h

rsc.li/materials-advances

Introduction

Polymer nanofibers have attracted much attention as a key material for fabricating various functional devices, such as filters, batteries, fuel cells, sensors, and cell culture media, owing to their unique chemical and mechanical properties.[1–10] Numerous studies on the preparation of nanofibers based on various fabrication methods have been reported so far. Among them, electrospinning is one of the most widely investigated methods for fabricating polymer nanofibers.[11–13] In this method, a polymer droplet is drawn out under a high electric field between a nozzle and a substrate, thereby generating nanofibers. This method can be applied to various polymers and enables the efficient formation of polymer nanofibers with controlled diameters by changing the preparation conditions. However, the problem with this process is the difficulty in obtaining uniformly sized nanofiber diameters smaller than 50 nm. On the other hand, the spinning method using a spinneret is commonly used for preparing polymer fibers. This method enables the continuous formation of polymer fibers with uniform diameters from multiple apertures of the spinneret. It also enables the efficient fabrication of polymer fibers and is thus used widely for industrial production. In this method, the diameter of the obtained fibers is essentially determined by the diameter of the apertures of the spinneret. To obtain fine fibers, a spinneret with fine apertures is required. To solve this problem, we have investigated the spinning method using a nanohole array material, *i.e.*, anodic porous alumina, as a spinneret. Anodic porous alumina, which is fabricated *via* the anodic oxidation of an Al substrate in an electrolyte, is a suitable spinneret material for a making polymer nanofibers with controlled diameters owing to the uniformity of the holes and controllability of the hole diameter from 10 nm to 1 μm.[14,15] We have reported that polymer nanofibers with uniform diameters can be obtained by extruding a polymer solution through holes of anodic porous alumina into a solidifying solution, and that the diameter of the obtained polymer nanofibers can be controlled by changing the hole diameter of the anodic porous alumina spinneret.[16,17] In this process, for obtaining fine nanofibers, the aperture diameter has to be reduced. The problem to be solved, accompanied by the reduction in the aperture diameter, is that the pressure loss increases in the direction of depth in the spinneret. The increase in pressure loss makes it difficult to extrude the polymer solution. This is a serious problem, especially in the case of highly viscous polymer solutions. To overcome this problem, we have developed new types of anodic porous alumina spinnerets with holes of different

Department of Applied Chemistry, Tokyo Metropolitan University, 1-Minamiosawa, Hachioji, Tokyo 192-0397, Japan. E-mail: yanagish@tmu.ac.jp

diameters in the direction of its thickness. In the spinneret with holes of different diameters, the layer with fine holes acts as an aperture layer for extrusion of the polymer solution, and the layer with larger holes acts as a support layer. By adopting the spinneret with a two-layered hole array structure, we can realize extrusion with both a low pressure loss and a reduced hole diameter.

In this work, two types of porous alumina spinneret with holes of different diameters were prepared: one is a spinneret prepared using a process involving anodization and a sub sequent pore-widening treatment, and the other is a spinneret prepared *via* anodization under different anodization voltages. Although the preparation of anodic porous alumina spinnerets with holes of different diameters has previously been reported,[18,19] this is the first example of the use of porous alumina as the material for the spinnerets with holes of different diameters for spinning. In this work, using these new types of spinnerets, we were able to form extremely fine nanofibers of ~12 nm diameter. In addition, fine carbon nanofibers were also prepared through carbonization of the obtained nanofibers as a precursor. As the process described in this work provides good controllability of the diameters of the nanofibers based on the hole diameters of the spinneret as well as wide applicability to various types of polymer, it will contribute to the fabrication of various functional nanofibers that are required in various application fields.

Experimental

Fig. 1 shows the fabrication process for an anodic porous alumina membrane using a bilayer structure with holes of different diameters as the spinneret. In this study, anodic porous alumina membranes were prepared using the following two processes. In the first process, the hole diameter is modulated without changing the interhole distance of the anodic porous alumina (Fig. 1(a)). In the other process, the hole diameter is modulated by varying the interhole distance of the anodic porous alumina (Fig. 1(b)). To fabricate anodic porous alumina with uniformly sized holes *via* both methods, ordered anodic porous alumina was prepared on the basis of our previously reported two-step anodization process.[20] Our previous study has shown that anodic porous alumina has holes of more uniform diameters and shapes as the regularity of the hole arrangement increases.[21] First, Al plates (99.99% in purity) that were electropolished using perchloric acid and ethanol (1 : 4 in volume ratios) at 0.1 A cm^{-2} for 4 min were anodized for 17 h in 0.3 M oxalic acid at 17 °C under a constant voltage of 40 V. As a result of this treatment, the arrangement of holes at the bottom of the anodic porous alumina becomes self-organized and regular. The oxide film formed by the long-term anodization was selectively dissolved by immersion of the sample in a mixed solution containing 6 wt% phosphoric acid and 1.8 wt% chromic acid at 70 °C for 4 h to obtain an Al plate with dimples. These dimples, which were regularly arranged on the surface, were the starting points for hole generation in the next anodization step. In both fabrication processes for anodic porous alumina samples, an Al plate with an ordered dimple pattern was used as the starting material.

Fig. 1(a) shows a schematic of the preparation process for anodic porous alumina with a bilayer structure that contains holes of different diameters without changing the interhole distance. Anodic porous alumina with a bilayer structure was prepared through a combination of two anodization steps under the same voltage and pore-widening treatment. An Al plate with an ordered dimple pattern was anodized in 0.3 M oxalic acid for 3 h at 17 °C under a constant voltage of 40 V. This first anodization step generated anodic porous alumina with an interhole distance of 100 nm and a thickness of 20 μm, which acts as a support layer. After this first anodization, the sample was immersed in 10 wt% phosphoric acid at 30 °C for 25 min to increase the hole diameter. Then, the sample was anodized again for 90 s under the same conditions to form anodic porous alumina with an interhole distance of 100 nm without increasing the hole diameter. For exfoliation of the alumina membrane with a bilayer structure, a two-layer anodization process using concentrated sulfuric acid was carried out.[22,23] The sample was anodized in 12 M sulfuric acid at 0 °C for 25 min under a constant voltage of 40 V to form an extremely soluble alumina layer at the bottom of the film. The alumina layer formed in concentrated sulfuric acid shows high solubility owing to the large amount of sulfate anions incorporated into the film. After anodization of the sample in concentrated sulfuric acid, the alumina membrane was detached *via* the selective dissolution of the oxide layer formed in concentrated sulfuric acid. The etching of the sample was carried out in 6 wt% phosphoric acid and 1.8 wt% chromic acid at 30° for 10 min.

Fig. 1(b) shows a schematic of the preparation process for anodic porous alumina with a bilayer structure and holes of different diameters prepared by varying the interhole distance. The pre-textured Al plate was anodized in 0.3 M oxalic acid at 17 °C under a constant voltage of 40 V for 90 s to form anodic porous alumina with an interhole distance of 100 nm. The anodic porous alumina obtained by anodization is amorphous and highly soluble in acids, but crystallization *via* heat treatment can reduce its solubility. Therefore, to reduce the solubility of the obtained alumina layer, heat treatment was performed at 600 °C for 1 h. After the heat treatment, the sample was anodized in a mixture of 0.25 M phosphoric acid and 0.05 M oxalic acid at 0 °C under a constant voltage of 160 V for 20 h to form anodic porous alumina with an interhole distance of 400 nm at the bottom of the porous layer and an interhole distance of 100 nm at the top. The obtained anodic porous alumina with a bilayer structure was detached through anodization in 17.6 M sulfuric acid at 160 V for 1 h and subsequent etching in a mixture of phosphoric acid and chromic acid at 30 °C for 10 min. The detached alumina membrane was immersed in 10 wt% phosphoric acid at 30 °C for 1 h to increase the hole diameter of the porous layer with an interhole distance of 400 nm, so that this layer acts as a support layer with holes of large diameters.

The permeability of the alumina membranes with bilayer structures fabricated using the two different processes was evaluated by measuring the amount of distilled water that permeated under pressurized conditions using N_2 gas. Fig. 1(c) shows a schematic of the polymer nanofiber spinning

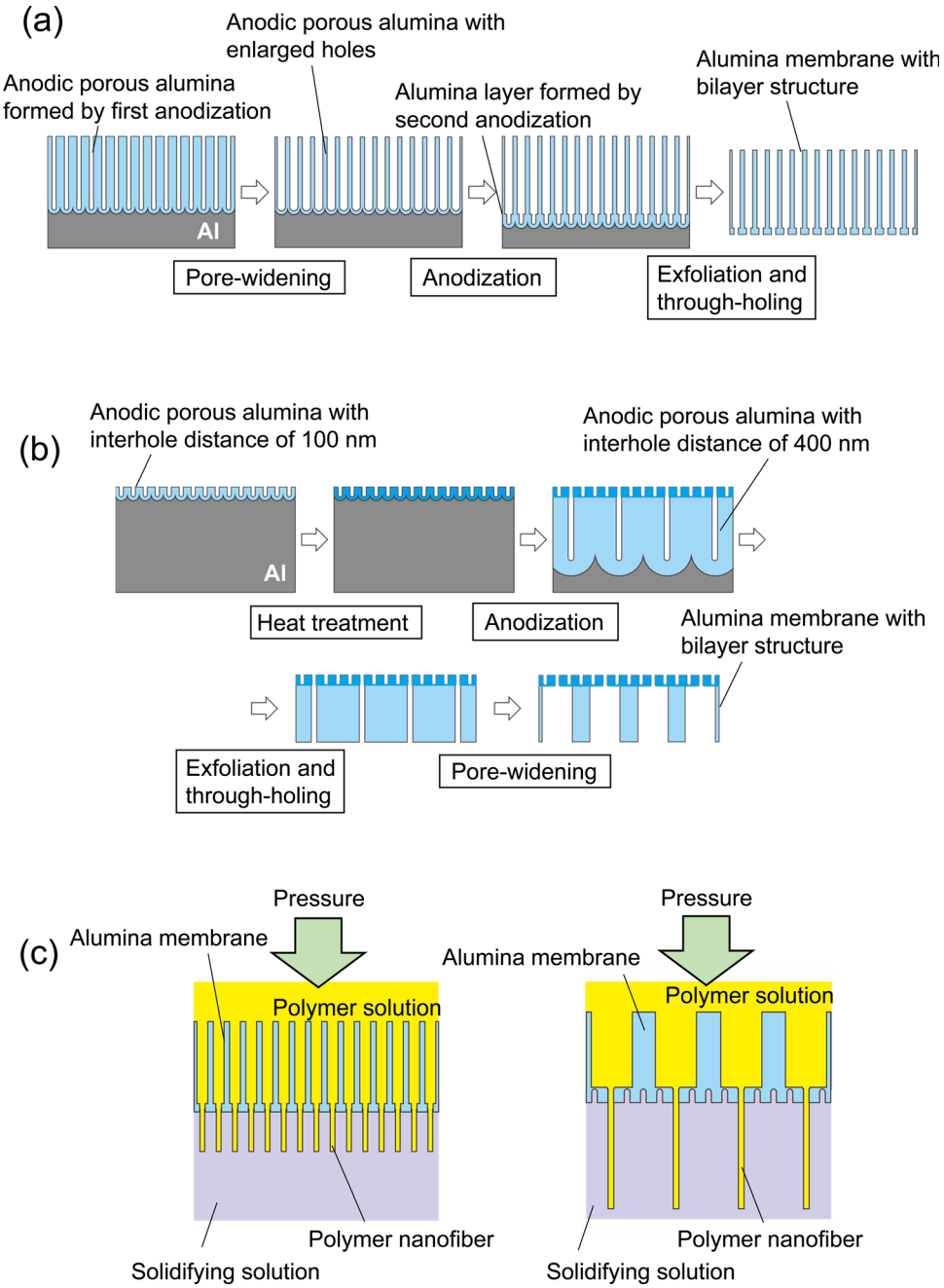

Fig. 1 Schematic of the preparation process for anodic porous alumina membranes with a bilayer structure and holes of different diameters obtained (a) without varying the interhole distance and (b) with varying the interhole distance. (c) Formation of polymer nanofibers *via* continuous spinning using anodic porous alumina membranes with bilayer structures.

method using anodic porous alumina spinnerets with bilayer structures. Dimethylformamide containing 7 wt% polyacrylonitrile was used as a polymer solution for spinning of the polymer nanofibers. Distilled water was used as a solidifying solution. The polymer solution was pressurized at 200–300 kPa using N_2 gas and extruded through the holes of the anodic porous alumina spinnerets into the solidifying solution. The polymer nanofibers extruded into the solidifying solution were picked up using tweezers attached to the desktop dip coater (DC4200, Aiden, Japan) and pulled up at a speed of 100 μm s^{-1} while spinning. The obtained samples were observed *via* scanning electron microscopy (SEM; JSM-7500F, JEOL). The hole diameter of the alumina spinnerets and the nanofiber diameters were evaluated by measuring the diameter distribution of 500 points from the SEM images.

Results and discussion

Fig. 2 shows SEM images of the anodic porous alumina spinneret with a bilayer structure and holes of different diameters

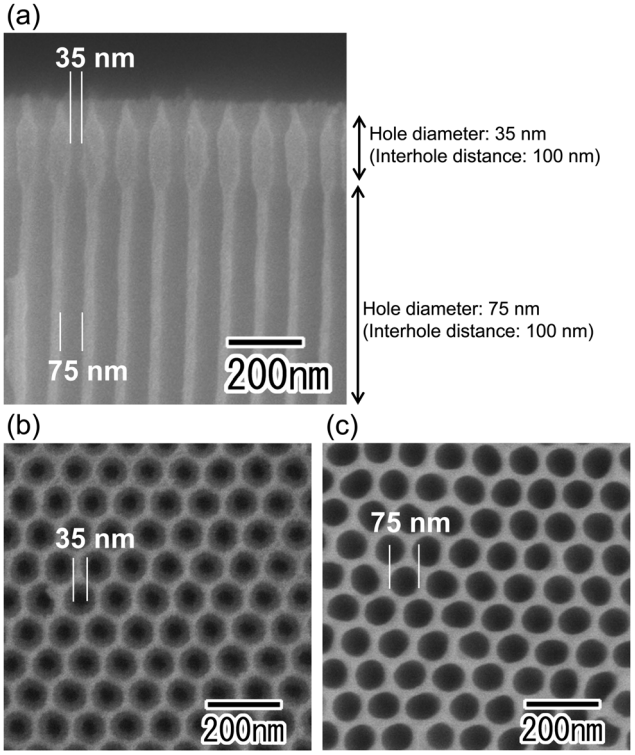

Fig. 2 SEM images of an anodic porous alumina membrane with a bilayer structure and holes of different diameters prepared using two anodization steps at the same anodizing voltage. SEM images of (a) the cross-section of the membrane, (b) the surface of the aperture layer for the extrusion of a polymer solution, and (c) the surface of the support layer.

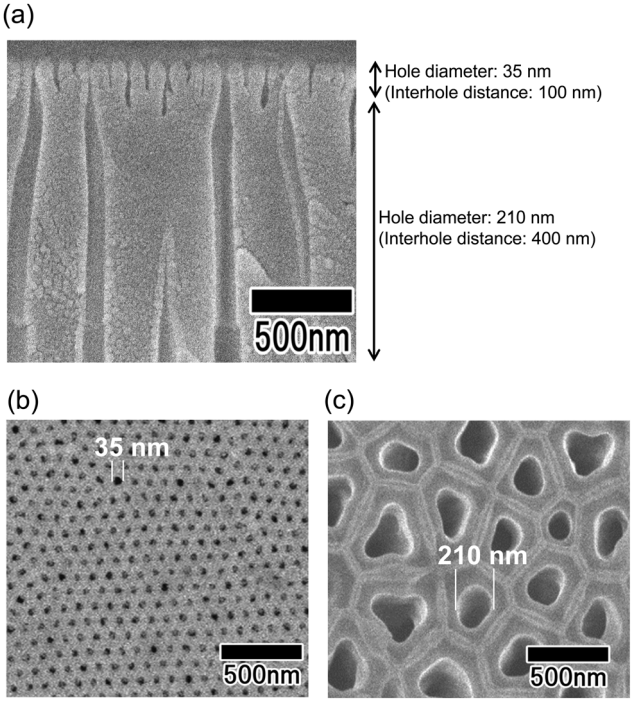

Fig. 3 SEM images of an anodic porous alumina membrane with a bilayer structure and holes of different diameters prepared using two anodization steps at different anodizing voltages. SEM images of (a) the cross-section of the membrane, (b) the surface of the aperture layer for the extrusion of a polymer solution, and (c) the surface of the support layer.

prepared without changing the interhole distance. The cross-sectional SEM image in Fig. 2(a) shows that the interhole distances of the upper and lower layers are both 100 nm, but the hole diameters are different. The hole diameters of the membranes were 35 and 75 nm, as shown in Fig. 2(b) and (c), respectively. However, this method has the problem that there is a limit to the modulation of the hole diameter because the two porous alumina layers have the same interhole distance. In general, the hole diameter of anodic porous alumina is about 30% of the interhole distance. Therefore, it is necessary to further reduce the interhole distance of the anodic porous alumina layer to reduce the diameters of the holes that collectively serve as the nozzle of the spinneret for polymer nanofiber formation. On the other hand, to improve the permeability of the anodic porous alumina spinneret, it is necessary to increase the hole diameter of the support layer to reduce the pressure loss. When a bilayer structure with holes of different diameters is prepared without changing the interhole distance, the hole diameter of the support layer cannot be increased beyond the interhole distance.

Fig. 3 shows SEM images of the anodic porous alumina spinneret with a bilayer structure and holes of different diameters prepared by varying the interhole distance. From the cross-sectional SEM image shown in Fig. 3(a), it can be observed that the interhole distance of the porous layer changes in the middle of the film because the sample was prepared by carrying out anodization twice at different voltages. The interhole distance of anodic porous alumina varies depending on the anodization voltage, and a linear relationship of 2.5 nm V^{-1} is established between these two factors. For preparation of the sample shown in Fig. 3, the anodization voltage was changed from 40 to 160 V, and the interhole distance of the porous layers was observed to change from 100 to 400 nm. The hole diameters of the anodic porous alumina spinneret, as measured from the SEM images shown in Fig. 3(b) and (c), were 35 and 210 nm, respectively. Since the solubility of the surface layer was reduced by heat treatment before the support layer formation, the small hole diameter of the alumina layer with an interhole distance of 100 nm was maintained even after the wet etching treatment to increase the hole diameter in the support layer.

Fig. 4 shows results of the water permeability of the anodic porous alumina membranes with the two types of bilayer structure obtained in this study. For comparison, the results for an anodic porous alumina membrane without hole diameter modulation are also shown in Fig. 4. Since the hole density varies with the interhole distance of the anodic porous alumina, the permeability of each alumina membrane was evaluated by calculating the permeation performance of a single hole as follows: the amount of water that flowed through the alumina holes divided by the number of holes. Although the surface hole diameter of all three types of alumina membrane used in this experiment is 35 nm, the alumina membrane with the hole diameter modulation has a higher

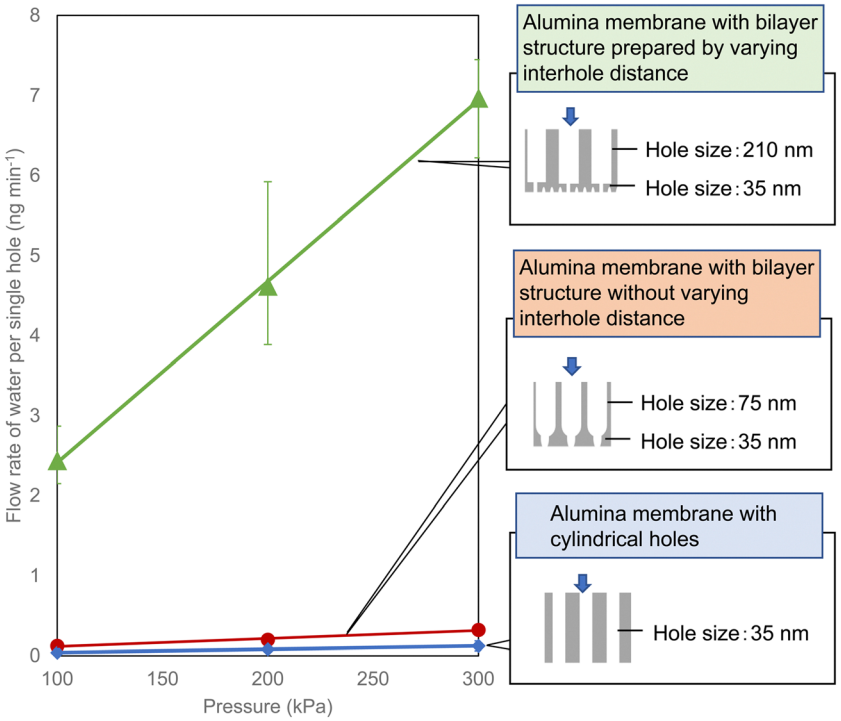

Fig. 4 Flow rate of water per hole in anodic porous alumina membranes with three types of structure.

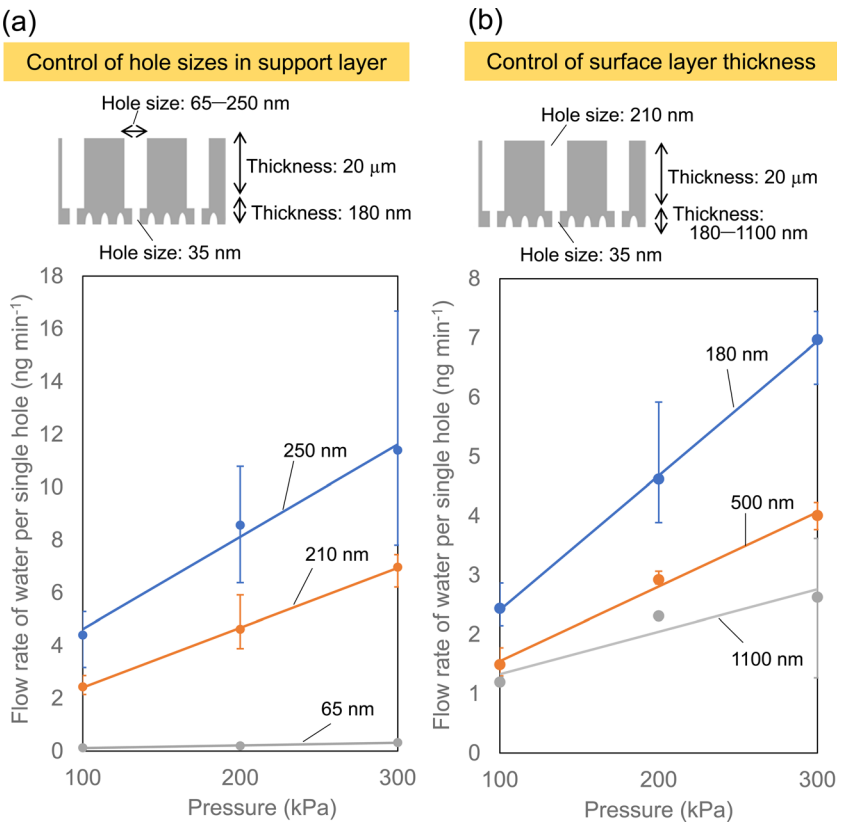

Fig. 5 (a) Water permeation properties of anodic porous alumina membranes with a bilayer structure and holes of different diameters in the support layer. (b) Solution permeation properties of the anodic porous alumina membranes with a bilayer structure and holes of different depths in the fine hole layers.

water permeability than the alumina membrane with cylindrical holes prepared without hole diameter modulation. This result indicates that alumina membranes with hole diameter modulation have improved permeation properties because the extent of the pressure drop is reduced owing to the enlarged holes of the support layer. It was also found that the alumina membrane with various interhole distances exhibited a higher permeability than the alumina membrane with a constant interhole distance. The reason for this is considered to be as follows: the hole diameter of the support layer is larger in the alumina membrane with variation of the interhole distance than in the alumina membrane prepared without varying the interhole distance.

Fig. 5 shows the effect of the porous structure of the alumina membrane on the water permeation properties. In this experiment, a porous alumina membrane with a bilayer structure having different interhole distances, which exhibited the highest solution permeability as shown in Fig. 4, was used. Anodic porous alumina with a bilayer structure with holes of different diameters was prepared *via* anodization at 40 and 160 V. The interhole distances were 100 and 400 nm, respectively. Fig. 5(a) shows the results of an experiment to study the effect of the hole diameter of the support layer on the solution permeability. The bilayer alumina membranes used in this experiment were prepared to have a fixed hole diameter of 35 nm and a fixed hole depth of 180 nm in the upper alumina layer. In addition, the hole depth in the support layer was fixed at 20 μm. Fig. 5(a) shows that the flow rate of water per hole increases with the hole diameter of the support layer. This is considered to be due to the pressure loss during solution permeation being smaller when the hole diameter of the support layer is larger. Fig. 5(b) shows the results of an experiment on the effect of the depth of the fine holes in the upper alumina layer on the water permeability. In this experiment, the hole diameter in the upper alumina layer with different the hole depths was fixed at 35 nm, whereas the thickness and hole diameter of the support layer were fixed at 210 nm and 20 μm, respectively. The hole depth for the upper alumina layer with a hole diameter of 35 nm was controlled at 180, 500, and 1100 by adjusting the anodization time. Fig. 5(b) shows that the water permeability can be increased by making the hole depth smaller in the porous alumina layer with a hole diameter of 35 nm. These results indicate that it is important to control the hole diameter in the support layer to be large and the depth of smaller holes to be smaller to increase the solution permeability.

Fig. 6 shows the SEM image and diameter distribution histogram of polymer nanofibers obtained *via* continuous spinning. For this sample, the anodic porous alumina membrane having a bilayer structure with interhole distances of 100 and 500 nm was used as the spinneret. The support layer of the anodic porous alumina spinneret was prepared by anodization in 0.1 M phosphoric acid at 0 °C under a constant voltage of 200 V for 8 h. The alumina membrane was detached by anodization of the sample in 17.6 M sulfuric acid at 200 V for 1 h followed by etching in a mixture of phosphoric and chromic acids.[23] After detachment of the alumina membrane, the holes of the support layer were enlarged using a pore-widening treatment in 10 wt% phosphoric acid. The hole diameters of the anodic porous alumina spinneret used for spinning the

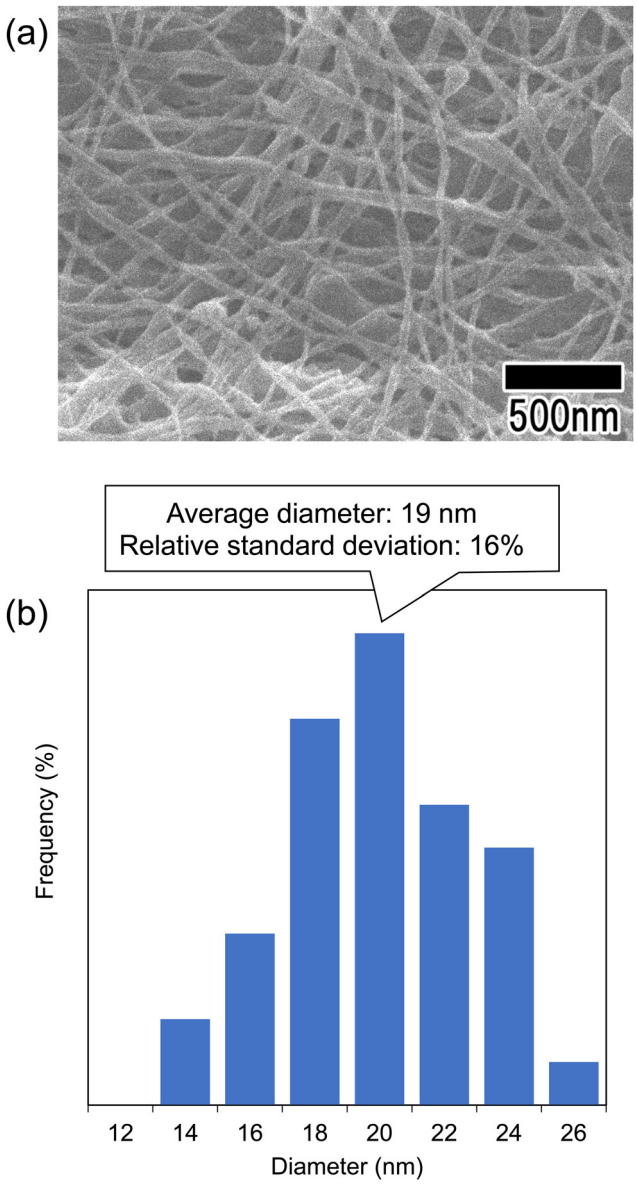

Fig. 6 (a) SEM image of the polymer nanofibers obtained *via* continuous spinning using anodic porous alumina with a bilayer structure. (b) Diameter distribution histogram of the obtained nanofibers.

polymer nanofiber shown in Fig. 6 were 28 and 250 nm. The thicknesses of the surface and support layers were 180 nm and 20 μm, respectively. The SEM image in Fig. 6(a) shows that polymer nanofibers were formed with a generally uniform diameter. The diameter distribution histogram in Fig. 6(b) confirmed that the average diameter of the obtained polymer nanofibers was 19 nm and the relative standard deviation, which indicates the variation of the obtained nanofibers, was 16%. Conventional anodic porous alumina membranes with cylindrical holes could not extrude highly viscous polymer solutions when the diameter was set to less than 30 nm, making it difficult to spin polymer nanofibers. However, using anodic porous alumina with a bilayer structure containing holes of different diameters, we were able for the first time to

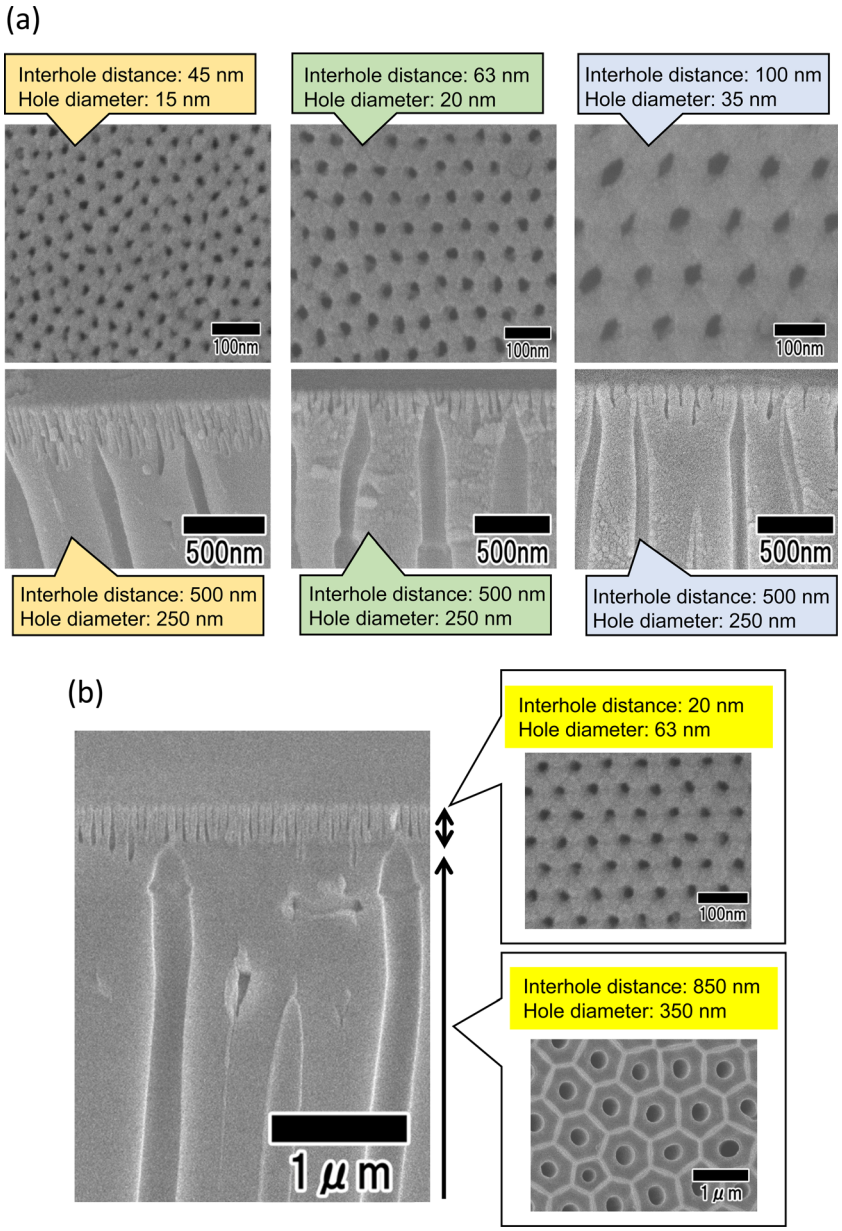

Fig. 7 (a) SEM images of anodic porous alumina membranes with bilayer structures with controlled surface interhole distances. (b) SEM images of an anodic porous alumina membrane with a bilayer structure and interhole distances of 63 and 850 nm.

form polymer nanofibers from holes with diameters of less than 30 nm.

Using this method, it is also possible to further reduce the surface hole diameter by reducing the interhole distance of the anodic porous alumina layer formed on the surface of its bilayer structure. Fig. 7(a) shows SEM images of an anodic porous alumina membrane that has a bilayer structure with an interhole distance of 500 nm in the support layer and interhole distances of 45, 63, and 100 nm on the surface. The ordered anodic porous alumina layer on the top surface was fabricated under the previously reported anodization conditions at 18, 25, and 40 V, respectively.[14,23,24] The cross-sectional SEM images of all the samples show that the interhole distance changes in the middle of the film. In all the samples, the hole diameter of the support layer is 250 nm, whereas the hole diameters of the surface layer are 15, 20, and 35 nm, respectively, indicating that as the interhole distance decreases, the hole diameter also decreases. Fig. 7(b) shows the results of increasing the interhole distance of the support layer to 850 nm to further increase the diameter of the support layer. The support layer was prepared *via* anodization in a mixture of 0.2 M citric acid and 2 mM phosphoric acid at 16 °C under a constant voltage of 340 V for 8 h. Anodization using concentrated sulfuric acid to detach the membrane was performed in 17.6 M sulfuric acid at 0 °C under a constant voltage of 340 V for 1 h. The hole diameter of the support layer was increased by immersing the sample in

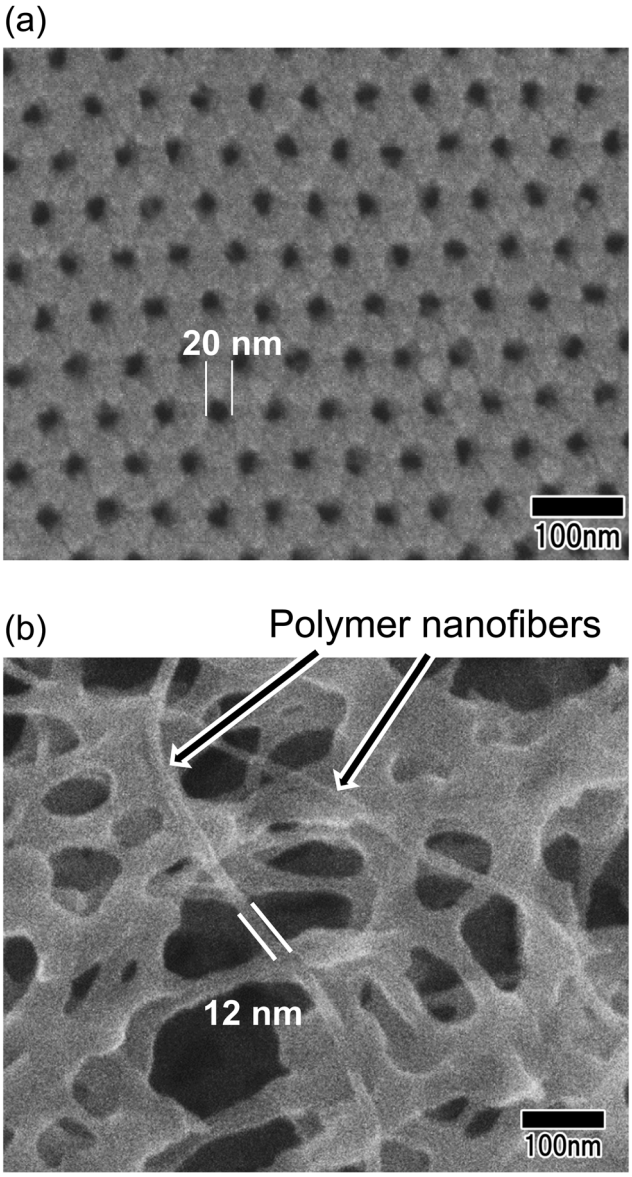

Fig. 8 (a) Surface SEM image of an anodic porous alumina membrane used as a spinneret. (b) SEM of polymer nanofibers obtained *via* continuous spinning using an anodic porous alumina spinneret.

20 wt% phosphoric acid at 30 °C for 1 h. The SEM images in Fig. 7(b) show the formation of an anodic porous alumina membrane with a hole diameter of 20 nm in the surface layer and a hole diameter of 350 nm in the support layer. These results indicate that the hole diameters of the surface and support layers can be controlled by changing the anodization voltage and the subsequent pore-widening.

Fig. 8 shows the SEM image of polymer nanofibers fabricated *via* continuous spinning using an anodic porous alumina membrane as the spinneret with a bilayer structure with a hole diameter of 20 nm in the surface layer and a hole diameter of 340 nm in the support layer. The diameter of the resulting polymer nanofibers was 12 nm, but at the present stage, the polymer nanofibers were only partially formed owing to insufficient optimization of the spinning conditions. Polymer nanofibers with a diameter of 12 nm are the finest nanofibers obtained by the spinning process using anodic porous alumina as a spinneret. These results indicate that even when an anodic porous alumina membrane with a bilayer structure is used as the spinneret, the diameter of polymer nanofibers can be reduced by decreasing the hole diameter on the surface of the alumina membrane.

Fig. 9 shows the average diameters of polymer nanofibers obtained using three different types of anodic porous alumina spinneret: a spinneret with cylindrical holes, a spinneret with a bilayer structure prepared without varying the interhole distance, and a spinneret with a bilayer structure prepared with the interhole distance varied. A linear relationship was observed between the surface hole diameters of the three types of anodic porous alumina used as the spinneret and the average diameters of the polymer nanofibers. This result means that the diameter of the polymer nanofibers obtained *via* continuous spinning using anodic porous alumina as the spinneret varies only with the surface hole diameter and not with the internal structure of the alumina membrane. From the results obtained in this study, we conclude that by controlling the shape of the holes and minimizing the pressure drop, it is possible to produce fine polymer nanofibers because the highly viscous polymer solutions are extruded through the alumina holes even when the hole diameter is reduced. In the future, it is expected that controlling the membrane structure will lead to an efficient fabrication method for fabricating polymer nanofibers with controlled diameters in the single-digit nanometer range.

Finally, as an application of the polymer nanofibers obtained in this study, the preparation of carbon nanofibers was investigated. This method can produce nanofibers composed of polyacrylonitrile, which is an effective raw material for carbon fibers. Therefore, if the nanofibers obtained using this method can be carbonized, it is expected that this method will be applicable to the efficient preparation of carbon nanofibers with controlled diameters. Fig. 10 shows SEM images and Raman spectra of polymer nanofibers obtained before and after heat treatment. Heat treatment was performed in air at 250 °C for 2 h, then the temperature was increased at a rate of 5 °C min^{-1} in an N_2 atmosphere, held at 1000 °C for 1 min, and then allowed to cool. The SEM images in Fig. 10(a) and (b) show that the nanofiber structure is maintained even after heat treatment. The Raman spectrum of the annealed sample shows that a peak originating from graphite (G-band), which was not observed before annealing, was observed at around 1590 cm^{-1}, and a peak originating from the defect structure of graphite (D-band) was also observed at 1350 cm^{-1}. Although we were unable to obtain fully graphitized nanofibers owing to the limitation of the equipment used for the heat treatment, which did not allow heat treatment above 1000 °C, carbon nanofibers with a uniform diameter were obtained *via* heat treatment in an N_2 atmosphere. There have been several reports on the fabrication of carbon nanofibers with diameters of 50 nm or less. For example, it has been reported that the carbonization of cellulose and agarose can form carbon

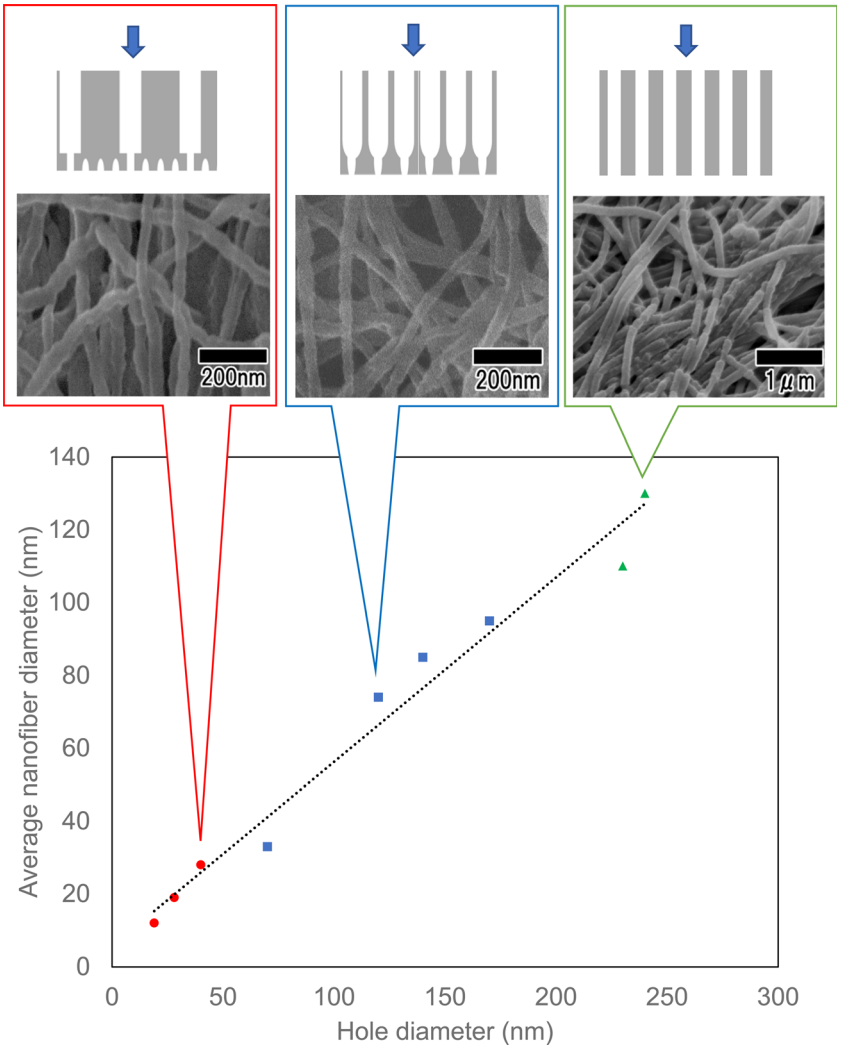

Fig. 9 Summary of the average diameters of polymer nanofibers obtained using three different types of anodic porous alumina spinneret.

nanofibers with a diameter of 10–20 nm.[25,26] However, it is difficult to control the diameter of the resulting carbon nanofibers using this method. Although it has also been reported that carbon nanofibers with a diameter of 20–30 nm can be obtained *via* chemical vapor deposition synthesis using metal catalysts, the diameter uniformity of the obtained carbon nanofibers was low.[27] In contrast to these methods, our method reported here enables the formation of carbon nanofibers with uniform diameters, as well as the control over the diameter of the resulting nanofibers. The carbon nanofibers obtained using this process are expected to have various applications, for example, as materials for devices such as electrodes for electric double-layer capacitors.

Conclusions

Two types of bilayer anodic porous alumina structure with holes of different diameters were fabricated by controlling the anodization conditions. The measured flow rate of distilled water through the obtained anodic porous alumina membrane showed that the two types of alumina membrane with bilayer structures, in which the hole diameter in the support layer is increased, have a higher solution permeability than a conventional alumina membrane that has cylindrical holes. It was also found that anodic membranes with a bilayer structure prepared with various interhole distances exhibited a higher solution permeability than alumina membranes prepared without varying the interhole distance, because the hole diameter of the support layer could be further increased. Polymer nanofibers with uniform diameters were successfully spun using an anodic porous alumina spinneret with a bilayer structure containing holes of different diameters, and the average diameter of the polymer nanofibers was less than 20 nm. It was also confirmed that carbon nanofibers of uniform diameters were obtained when the polymer nanofibers were heat-treated in an N_2 atmosphere. Polymer and carbon nanofibers fabricated using this process are expected to be key materials for fabricating various functional devices, such as energy devices and biodevices.

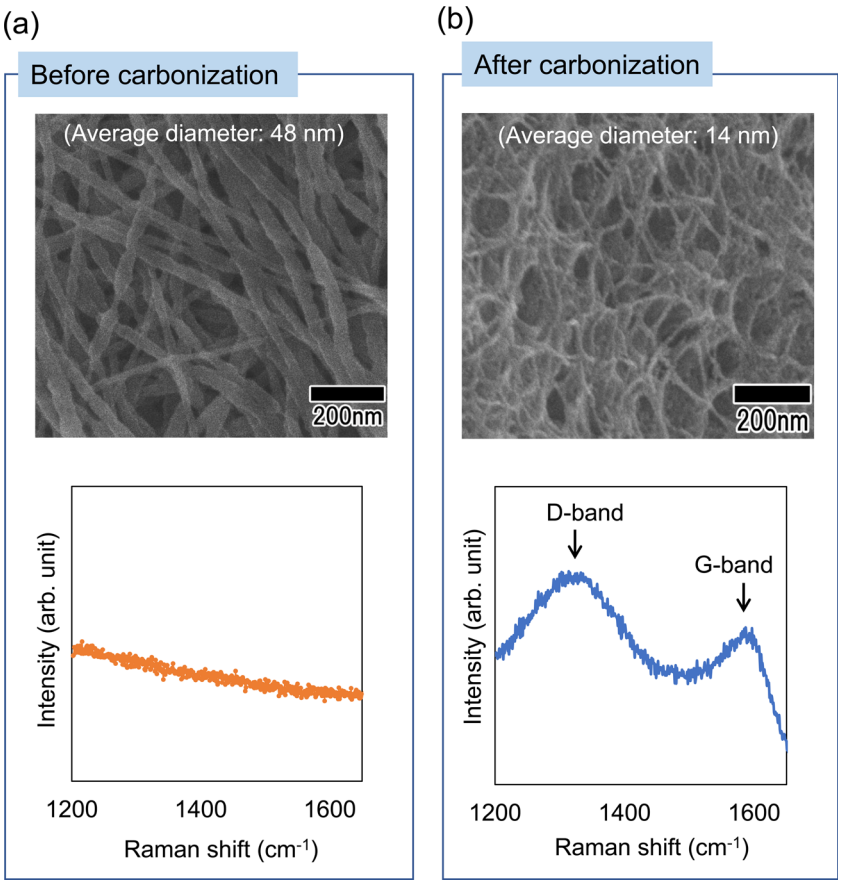

Fig. 10 SEM images and Raman spectra of the nanofibers (a) before and (b) after carbonization by heat treatment in an N_2 atmosphere.

Author contributions

T. Y.: conceptualization, methodology, investigation, writing – original draft;. A. K.: investigation; H. M.: writing – review and editing. All authors read and approved the manuscript.

Conflicts of interest

There are no conflicts to declare.

Acknowledgements

The present work was supported by JKA and its promotion funds from KEIRIN RACE.

References

1 F. E. Ahmed, B. S. Lalia and R. Hashaikeh, *Desalination*, 2015, **356**, 15.
2 H. Shao, J. Fang, H. Wang and T. Lin, *RSC Adv.*, 2015, **5**, 14345.
3 Q. Yao, J. G. L. Cosme, T. Xu, J. M. Miszuk, P. H. S. Picciani, H. Fong and H. Sun, *Biomaterials*, 2017, **115**, 115.
4 S. Cheon, H. Kang, H. Kim, Y. Son, J. Y. Lee, H. Shin, S. Kim and J. H. Cho, *Adv. Funct. Mater.*, 2018, **28**, 1703778.
5 Y. Kim and Y. T. Matsunaga, *J. Mater. Chem. B*, 2017, **5**, 4307.
6 A. Barhoum, K. Pal, H. Rahier, H. Uludag, I. S. Kim and M. Bechelany, *Appl. Mater. Today*, 2019, **17**, 1.
7 A. S. Levitt, M. Alhabeb, C. B. Hatter, A. Sarycheva, G. Dion and Y. Gogotsi, *J. Mater. Chem. A*, 2019, **7**, 269.
8 S. Jafari, S. S. H. Salekdeh, A. Solouk and M. Yousefzadeh, *Polym. Adv. Technol.*, 2020, **31**, 284.
9 W. Liang, Y. Xu, X. Li, X. Wang, H. Zhang, M. Yu, S. Ramakrishna and Y. Long, *Nanoscale Res. Lett.*, 2019, **14**, 361.
10 G. J. Kim and K. O. Kim, *Sci. Rep.*, 2020, **10**, 18858.
11 Z. Li, H. Zhang, W. Zheng, W. Wang, H. Huang, C. Wang, A. G. MacDiarmid and Y. Wei, *J. Am. Chem. Soc.*, 2008, **130**, 5036.
12 K. Brezesinski, R. Ostermann, P. Hartmann, J. Perlich and T. Brezesinki, *Chem. Mater.*, 2010, **22**, 3079.
13 F. Li, Z. Kang, X. Huang and G. Zhang, *Chem. Eng. J.*, 2013, **234**, 184.
14 H. Masuda and K. Fukuda, *Science*, 1995, **268**, 1466.
15 T. Yanagishita, R. Moriyasu, T. Ishii and H. Masuda, *RSC Adv.*, 2021, **11**, 3777.

16 T. Yanagishita, H. Awata, K. Kobayashi, T. Kondo and H. Masuda, *Chem. Lett.*, 2019, **48**, 86.
17 T. Yanagishita, H. Takai, T. Kondo and H. Masuda, *Nanotechnology*, 2021, **32**, 145603.
18 X. Zhu, Y. Song, D. Yu, C. Zhang and W. Yao, *Electrochem. Commun.*, 2013, **29**, 71.
19 L. Zaraska, E. Kurowska, G. D. Sulka and M. Jaskula, *J. Solid State Electrochem.*, 2012, **16**, 3611.
20 H. Masuda and M. Satoh, *Jpn. J. Appl. Phys.*, 1996, **35**, L126.
21 T. Yanagishita, K. Murakoshi and H. Masuda, *ECS J. Solid State Sci. Technol.*, 2022, **11**, 103004.
22 T. Yanagisihta and H. Masuda, *Electrochim. Acta*, 2015, **184**, 80.
23 T. Yanagishita, M. Ozaki, R. Kawato, A. Kato, T. Kondo and H. Masuda, *J. Electrochem. Soc.*, 2020, **167**, 163502.
24 H. Masuda, M. Nagae, T. Morikawa and K. Nishio, *Jpn. J. Appl. Phys.*, 2006, **45**, L406.
25 E. Jazaeri, L. Zhang, X. Wang and T. Tsuzuki, *Cellulose*, 2011, **18**, 1481.
26 Z. Zhang, Y. Yu, C. Yao, Z. Li, G. Suo, J. Wu, X. Wang, M. Zhi and Z. Hong, *J. Nanopart. Res.*, 2018, **20**, 249.
27 W. Yan-li, W. Xu-jian, Z. Liang, Q. Wen-ming, L. Xiao-yi and L. Li-cheng, *New Carbon Mater.*, 2012, **27**, 153.